NACA

RESEARCH MEMORANDUM

AN EXPERIMENTAL INVESTIGATION OF THE EFFECT OF HIGH-PRESSURE TAILPIPE LENGTH ON THE PERFORMANCE OF SOLID-PROPELLANT MOTORS FOR ROCKET-POWERED AIRCRAFT

By Charles J. Rodriguez

Langley Aeronautical Laboratory
Langley Field, Va.

NATIONAL ADVISORY COMMITTEE FOR AERONAUTICS

WASHINGTON
August 12, 1952
Declassified May 8, 1957

NATIONAL ADVISORY COMMITTEE FOR AERONAUTICS

RESEARCH MEMORANDUM

AN EXPERIMENTAL INVESTIGATION OF THE EFFECT OF HIGH-PRESSURE TAILPIPE LENGTH ON THE PERFORMANCE OF SOLID-PROPELLANT MOTORS FOR ROCKET-POWERED AIRCRAFT

By Charles J. Rodriguez

SUMMARY

The effect of high-pressure tailpipe exhaust ducts having ratios of length to inside diameter L/D of 0, 5, 10, and 15 on the performance of solid-propellant rocket motors has been evaluated from thrust-stand tests. Boundary-layer development is found to reduce the effective nozzle throat area, for mass-flow considerations, from its value for $\frac{L}{D} = 0$ by 3.3 percent for $\frac{L}{D} = 5$, 5.1 percent for $\frac{L}{D} = 10$, and 6.4 percent for $\frac{L}{D} = 15$. Development of the boundary layer is found not to be proportional to pipe length but to diminish, apparently because of heat extraction, for increasing L/D ratios. A direct result of the reduction of effective throat area is an increase in chamber pressure, the magnitude being dependent on the type of propellant burned. For JPN, the composition used in the present investigation, the increases in chamber head pressure over that obtained for $\frac{L}{D} = 0$ are 13.4 percent for $\frac{L}{D} = 5$, 21.4 percent for $\frac{L}{D} = 10$, and 27.6 percent for $\frac{L}{D} = 15$. Higher operating pressures result in a decrease in burning time of 8.8 percent for $\frac{L}{D} = 5$, 13.2 percent for $\frac{L}{D} = 10$, and 16.3 percent for $\frac{L}{D} = 15$, and increases in the mass rate of flow of 9.6 percent for $\frac{L}{D} = 5$, 15.2 percent for $\frac{L}{D} = 10$, and 19.5 percent for $\frac{L}{D} = 15$. Friction and heat transfer result in duct losses but these are completely overwhelmed by the increase in chamber pressure so that resultant average thrust increases of 6.4 percent for $\frac{L}{D} = 5$, 10.9 percent for $\frac{L}{D} = 10$, and

14.2 percent for $\frac{L}{D} = 15$ are obtained. Duct losses become evident, however, in reductions of total and specific impulse from their values for $\frac{L}{D} = 0$. These average 3.0 percent for $\frac{L}{D} = 5$, 3.7 percent for $\frac{L}{D} = 10$, and 4.4 percent for $\frac{L}{D} = 15$.

INTRODUCTION

Rocket-powered aircraft using solid-propellant rocket motors as propulsive units pose a problem not usually encountered in types of aircraft employing liquid fuels. In the latter type, the combustion chamber and nozzle may be placed at the tail end of the aircraft, for proper jet clearance, and the separate fuel tanks conveniently installed elsewhere in the fuselage to achieve a desired center-of-gravity location. The solid-propellant type, however, is characterized by a fuel supply which is an integral part of the combustion chamber and no such distribution of component parts is possible. Forward positioning of the rocket motor due to center-of-gravity considerations results in a need for a duct to convey the rocket exhaust gases to the tail end of the fuselage. Ducts used for such purposes are called tailpipes or blast tubes. A low-pressure tailpipe consists of a cylindrical, constant-area duct attached to the exit section of a convergent-divergent nozzle. It conveys gases at low pressures and supersonic velocities. A high-pressure tailpipe consists of a cylindrical, constant-area duct inserted between the convergent and divergent sections of a nozzle. It forms, in effect, an extension of the nozzle throat and conveys gases at high pressures and velocities in the vicinity of sonic speed.

The high gas velocities, temperature, and, in the case of high-pressure tailpipes, pressures which tailpipes are subjected to during rocket operation influence the nature of the aerodynamic and thermodynamic losses within the duct. Attendant boundary-layer development will also affect rocket operation. The consequent effects of these factors upon rocket performance parameters such as burning time, operating pressure, thrust, mass rate of flow, and specific impulse are of interest to the rocket designer. Results of tests of low-pressure tailpipes are reported in reference 1. The present investigation, conducted by the Langley Pilotless Aircraft Research Division, is concerned with the effect of the variation of high-pressure tailpipe length-to-diameter ratio on solid-propellant rocket-motor performance.

SYMBOLS

A	geometrical cross-sectional area, sq in.
A'	effective cross-sectional area, sq in.
b	burning rate, in./sec
C_D	discharge coefficient, sec^{-1}
C_F	thrust coefficient
c	coefficient in burning rate equation
D	geometrical inside diameter of tailpipe, in.
F	thrust, lb
g	acceleration due to gravity, ft/sec/sec
H	boundary-layer shape parameter
I	total impulse, lb-sec
I_S	specific impulse lb-sec/lb fuel
K	ratio of burning surface to throat area
L	length of tailpipe, in.
M	free-stream Mach number
$\dot{m}$	instantaneous mass rate of flow, lb/sec
$\bar{\dot{m}}$	average mass rate of flow, lb/sec
m_g	rate of gas generation, lb/sec
n	exponent in burning rate equation
P	static pressure, lb/sq in. abs
R	gas constant, ft/$^{\circ}$R
R_e	Reynolds number

r	geometrical inside radius of tailpipe, in.
S	burning surface, sq in.
T	free-stream temperature, $^{\circ}R$
t	time, sec
t_b	burning time, sec
V	free-stream velocity, ft/sec
w	expended weight of propellant, lb
γ	ratio of specific heats
δ^*	displacement thickness, in.
θ	momentum thickness, in.
ρ	free-stream density, lb/cu in.
ρ'	density of solid propellant corrected for gas density in chamber, lb/cu in.

Subscripts:

A	space average
a	atmospheric
E	exit
H	head (closed) end of chamber
N	nozzle end of chamber
T	throat

APPARATUS AND TESTS

Simple convergent nozzles as illustrated in figure 1(a) were tested as the $\frac{L}{D} = 0$, or reference, runs. Three such tests were made.

High-pressure tailpipes as illustrated in figure 1(b) were formed by attaching ducts of equal and constant inside diameter to the throat section of similar convergent nozzles. The length of these ducts was varied to provide L/D ratios of 5, 10, and 15. Two tests of each L/D ratio were made.

The mass of metal present to extract heat from the gas stream will undoubtedly affect duct losses and, to be consistent in keeping L/D the only variable, this mass must vary only through changes in pipe length, not wall thickness. All tailpipes were consequently of $\frac{3}{16}$-inch wall thickness, for it was determined from previous firings of high-pressure tailpipes that this was the minimum practical thickness for structural considerations.

For all tests, the divergent section was eliminated for ease of fabrication, since only an absolute evaluation of the effect of extending the nozzle throat was desired.

Navy HVSR, Mk. 3, rocket motors employing cruciform-shaped JPN propellant were used in all tests. Since the initial propellant temperature is an important factor in the determination of the burning rate of the powder, every effort was made to fire all charges at the same temperature, 70° F. The rocket motors were assembled and conditioned for approximately 5 hours in a temperature-controlled box to a temperature of 70° F.

Static-thrust time histories were obtained for each run by firing the rocket motors mounted in a thrust stand where the deflection of a beam, proportional to the thrust exerted, was measured by electrical strain gages and a recording galvanometer. Pressures at the forward and rearward ends of the chamber and at the exit section of each tailpipe were measured and similarly recorded using electrical pressure transmitters which convert pressure impulses to electrical impulses by means of electrical strain gages. Timing marks were indicated on the records by an electrical timer incorporated in the system.

PRELIMINARY OBSERVATIONS

Figures 2 to 5 show typical thrust and pressure time histories for each run. The abrupt change of slope near the end of each run indicates the cessation of orderly burning and any succeeding reaction is considered to be made up of the burning of small particles of powder left in the chamber and the exhaust of the combustion gases. Only the portions of each run up to this time, termed the "burning time" and indicated by a dashed line on each figure, are considered in this investigation.

Figure 6 is a cross plot of the data presented in figures 2 to 5.

Additional information pertinent to each run may be found in tables I and II. The values of the powder constants shown in table I were obtained from reference 2. The value of total impulse shown in table II is defined as

$$I = \int_0^{t_b} F \, dt \tag{1}$$

and the specific impulse as

$$I_S = \frac{I}{w} \tag{2}$$

where w, the expended weight of propellant in the burning time t_b, is taken as 98 percent of the original weight of the powder charge (ref. 3). Average thrusts and pressures shown are found directly from integration of the thrust and pressure time histories and the average mass rate of flow is given by

$$\bar{\dot{m}} = \frac{w}{t_b} \tag{3}$$

Consideration of these figures and tables reveals that the following preliminary observations may be made concerning the effect of tailpipe length on rocket performance:

(1) As the tailpipe length is increased, operating pressures, thrusts, and mass rates of flow increase and the burning time decreases.

(2) From figure 6, it may be seen that for any fixed value of operating pressure, increased tailpipe lengths yield decreasing values of thrust.

(3) The magnitude of this thrust loss at a fixed pressure decreases between subsequent runs as L/D is increased. In other words, duct losses are apparently greater in going from $\frac{L}{D} = 0$ to $\frac{L}{D} = 5$ than in going from $\frac{L}{D} = 5$ to $\frac{L}{D} = 10$ or from $\frac{L}{D} = 10$ to $\frac{L}{D} = 15$.

Additional observations which are not indicative of changes in performance due to the use of tailpipes, but which will affect analysis of the entire investigation are:

(1a) Due to inherent differences, even in powder grains taken from the same lot, the weights and burning surfaces of the charges varied slightly from run to run.

(2a) Due to metal erosion, the throat area changed during each run. A comparison of initial and final areas (after firing) is shown in table II and is manifested in figure 6 by the fact that the portion of each curve representing descending pressures does not coincide with that for ascending pressures. That this erosion undoubtedly progressed at a different rate for each L/D is implied by the variation of slopes between runs in figure 6 and by noting that the curves in figures 2 to 5 do not parallel each other.

(3a) The combined effect of (1a) and (2a) above is to cause appreciable variation in pressures, thrusts, mass rates of flow, and burning time even in runs of the same L/D. Specific impulse, a quantity which is independent of these variations, shows close agreement, however, for the three runs with $\frac{L}{D} = 0$.

(4a) For the tailpipe runs the specific impulse varies erratically with L/D and also shows scatter between runs of comparable L/D. In all cases but one it is higher in value than the specific impulse obtained for the reference runs $\left(\frac{L}{D} = 0\right)$. This is in contradiction to expectations, for duct losses must result in a decrease in specific impulse. A check shown in table II indicates that for all runs with tailpipes, final thrusts (at time t_b) per unit pressure, per unit throat area (as measured after firing) were higher than initial unit thrusts (at time 0.05 sec). This, coupled with the increases in specific impulse, points to an added phenomena encountered in the tailpipe runs - expansion beyond throat conditions, with subsequent higher exit velocities and hence impulse. This could be due to enlargement of the exit and formation of a throat inside the pipe as a result of erosion, or to a sudden decrease in boundary-layer thickness at the exit with consequent formation of an "effective" divergent section, or to a combination of both effects.

Examination of the tailpipes after firing revealed that in all cases they had eroded in the following way. Diameters after firing were largest at the nozzle entrance section and traveling downstream the diameter decreased gradually, until for about 1 inch before the exit it remained fairly constant. The exit itself was rounded off and it appeared that a slight "bell-mouthing" had taken place.[1] The final result was a long slightly convergent section with a small divergence at the exit.

---

[1]This condition had been specifically guarded against in the fabrication of the tailpipes and was not present at the start of any run.

In view of the larger final areas at the pipe entrances, and since the combustion gases are hottest in this region, it is not unreasonable to presume that erosion commenced at these sections first. Molten metal and scale from this region traveling down the pipe would serve to effectively reduce areas farther downstream - a condition which must have continued until these downstream sections became heated enough so that they too began to erode and increase in area. A sequence of events such as this could explain the fact that in figure 6 the initial ascending portion of each tailpipe run has a lower slope than the corresponding portion of the run with $\frac{L}{D} = 0$, indicating a reduction of some factor with time, probably throat area.[2] Later in each run, the slopes increase as was pointed out under 2a, undoubtedly coinciding with the start of erosion at downstream stations.

In summation, it is now evident that variables other than L/D have entered the investigation and must be accounted for in order to isolate the effect of tailpipe length on rocket performance. These variables are: differences in powder grain weight and burning surface, nozzle erosion, and, in the tailpipes, expansion beyond throat conditions.

ANALYSIS

Since all solid-fuel rocket motors operate at chamber pressures well above that required to exceed the critical pressure ratio, choking conditions exist at the minimum nozzle section or throat. For the simple rocket nozzle, if isentropic flow is assumed between the head (closed end) of the chamber where the Mach number is zero, and the nozzle throat where the Mach number is unity, the ratio of pressures between these two stations is

$$\frac{P_T}{P_H} = \left(\frac{2}{\gamma - 1}\right)^{\frac{\gamma}{\gamma-1}} \tag{4}$$

---

[2]Another investigator (ref. 4) found upon testing rockets with long ducts connecting chamber and nozzle (not an extended throat, but actually a "nozzle-entrance extension") that throat areas decreased during a run. He gives no adequate explantion of this phenomenon.

If free-stream properties are assumed to apply across the full geometrical cross section of the nozzle, the continuity equation defines the mass rate of flow as

$$\dot{m} = \rho V A \tag{5}$$

The energy and momentum equations lead to the equation for the thrust developed by a rocket motor (ref. 2)

$$F = \frac{\dot{m} V_E}{g} + (P_E - P_a) A_E \tag{6}$$

The first term of the right-hand side of equation (6) is the momentum thrust and the second term pressure thrust. Expansion of the gas to atmospheric pressure through a divergent section reduces the second term to zero and the increased thrust developed is due to the increased momentum of the jet.

Using the continuity equation (5), the perfect gas law

$$P = \rho R T \tag{7}$$

and expressing velocity in terms of Mach number and the speed of sound

$$V = M\sqrt{\gamma g R T} \tag{8}$$

equation (6) may be rewritten

$$F = \gamma P_E A_E M_E^2 + (P_E - P_a) A_E \tag{6a}$$

Thrust may also be written in terms of a thrust coefficient as

$$F = C_F A_T P_H \tag{9}$$

Combining equations (6a) and (9) it can be seen that thrust coefficient is defined as

$$C_F = \gamma \frac{P_E}{P_H} \frac{A_E}{A_T} M_E^2 + \frac{P_E}{P_H} \frac{A_E}{A_T} - \frac{P_a}{P_H} \frac{A_E}{A_T} \tag{10}$$

For the special case where the throat is the exit, as in a convergent nozzle, and $V_E = V_T$, $A_E = A_T$, $P_E = P_T$, and $M_E = M_T = 1$, equation (6a) may be written simply as

$$F = \gamma P_T A_T + \left(P_T - P_a\right) A_T \tag{6b}$$

and equation (10) as

$$C_F = \gamma \frac{P_T}{P_H} + \frac{P_T}{P_H} - \frac{P_a}{P_H} \tag{10a}$$

where the ratio P_T/P_H is defined by equation (4) for the isentropic case.

Equation (5) may be written in terms of a discharge coefficient as

$$\dot{m} = C_D A_T P_H \tag{11}$$

This discharge coefficient defines the mass rate of flow possible when a given powder composition is burned in a rocket motor having unit throat area and unit chamber head pressure. Ideally, it is a function only of the thermodynamic properties of the gas generated by combustion of that powder. However, due to factors such as incomplete combustion and heat transfer in the chamber, an experimental discharge coefficient will differ from this ideal. Since previous investigators have found that for the powder used in this investigation the discharge coefficient is constant throughout any run (ref. 5), C_D may be defined by integrating equation (11) to yield

$$C_D = \frac{w}{\int_0^{t_b} A_T P_H \, dt} \tag{12}$$

Substitution of experimental values in the right-hand side of equation (12) will then yield an experimental value of C_D.

Since the weight of propellant consumed in the burning time equals $\int_0^{t_b} \dot{m} \, dt$, specific impulse, from equations (1) and (2) may also be written

$$I_S = \frac{F}{\dot{m}} \tag{13}$$

When equation (13) is combined with equations (9) and (11), it will be seen that specific impulse is also given by

$$I_S = \frac{C_F}{C_D} \tag{14}$$

The burning rate of the powder is a function of the space average pressure in the chamber

$$b = cP_A^n$$

where the space average pressure is defined as (ref. 2)

$$P_A = \frac{2}{3} P_H + \frac{1}{3} P_N \tag{16}$$

The rate of gas generation is given in terms of burning surface, corrected powder density, and burning rate by

$$m_g = S\rho' b \tag{17}$$

and since to maintain equilibrium the rate of gas generation must equal the rate of discharge, equations (11) and (17) may be used to define the ratio of burning surface to effective throat area K as

$$K = \frac{S}{A_T} = \frac{C_D P_H}{\rho' b} \tag{18}$$

The space average pressure in the chamber is a function of the pressure drop from head to nozzle entrance, and, for a fixed chamber configuration, this drop should be about the same for all runs. The ratio P_A/P_H should therefore be the same also. In this investigation, P_A/P_H averaged 0.993. Using this factor and equation (15), equation (18) may be rewritten for the present runs as

$$K = \frac{C_D P_H^{1-n}}{c\rho'(0.993)^n} \tag{18a}$$

A powder grain parameter K has therefore been defined in terms of the thermodynamic properties of the gas and chamber head pressure. The former are constant for a particular powder composition so that K is seen to be a direct exponential function of pressure. Depending on the value of the exponent in the equation, slight changes in either of the factors making up K (S or A_T) may result in appreciable changes in pressure.

The equations just outlined served to define any quantity at any time that may be desired in the analysis of the runs with $\frac{L}{D} = 0$.

Flow through a high-pressure tailpipe, however, cannot be analyzed in the same fashion, for the long throat extension must introduce appreciable friction and heat-transfer effects. Any relation founded on isentropic flow between chamber and throat must be discarded.

Free-stream properties can no longer be assumed to apply across the full geometrical cross section. Friction forces slow down the flow in regions near the pipe walls, and, in effect, the main stream or core of flow may be considered as being thrust away from the physical walls by the boundary layer. The effective thickness of this boundary layer for mass-flow considerations is termed the displacement thickness δ^*.

The continuity equation must now take into account the mass-flow deficiency encountered in this boundary layer if it is to be written in terms of free-stream properties. The mass-flow deficiency is given by

$$\Delta\dot{m} = \rho V 2\pi r \delta^* \tag{19}$$

so that equation (5), for the tailpipe case, is modified to

$$\dot{m} = \rho V(A - 2\pi r \delta^*) \tag{5a}$$

From mass-flow considerations then, it may be seen that an effective throat area A_T' may be defined in terms of the geometrical throat area A_T as

$$A_T' = A_T - 2\pi r_T \delta_T^* \tag{20}$$

Though an effective throat be formed in a tailpipe by the boundary layer, rather than the physical walls, it must still, using free-stream properties and the powder constants already established, satisfy all equations previously established for the conventional nozzle. An effective throat area A_T' as defined by equation (20) must now be used in place of the geometrical throat area A_T in equations (5), (11), (12), and (18). (See summary of Consultation Memo 8, Dec. 1947, by H. S. Tsien in ref. 6, pp. 41-43.)

The thrust equation (6a), if it is to be written in terms of free-stream properties, must similarly be modified to account for the momentum thrust deficiency in the boundary layer. The effective thickness of the boundary layer for momentum thrust considerations is now increased over that used previously for mass-flow considerations by a factor termed the momentum thickness θ. The momentum thrust deficiency, as derived in the appendix, is given by

$$\Delta\dot{m}V = \rho V^2 2\pi r(\delta^* + \theta) \tag{21}$$

or

$$\Delta\dot{m}V = \gamma g P M^2 2\pi r(\delta^* + \theta) \tag{21a}$$

so that the thrust equation (6a), for the tailpipe case, is modified to

$$F = \gamma P_E M_E^2 \left(A_E - 2\pi r_E \delta_E^* - 2\pi r_E \theta_E\right) + \left(P_E - P_a\right) A_E \tag{6c}$$

No deficiency factor appears in the pressure thrust term of the thrust equation because pressure across the boundary layer is assumed uniform and equal to the pressure in the main stream, as is commonly done in boundary-layer investigations.

To arrive ultimately at an equitable comparison of the tailpipe and reference runs, it is necessary to solve for the value of throat pressure P_T for the tailpipe runs. It is not possible to proceed beyond the present point, however, without some assumptions. It is assumed, therefore, that the effective throat, although inside the pipe, is fairly near the exit and that isentropic relations may be used to link free-stream quantities between throat and exit. No assumption of isentropicity is made, it will be noted, for flow between chamber and throat, where it is believed that most losses occur.

The continuity equation in the form shown in equation (5a) is used to obtain the ratio of effective exit to effective throat area

$$\frac{A_E - 2\pi r_E \delta_E^*}{A_T - 2\pi r_T \delta_T^*} = \frac{M_T}{M_E}\left(\frac{1 + \frac{\gamma - 1}{2} M_E^2}{1 + \frac{\gamma - 1}{2} M_T^2}\right)^{\frac{\gamma+1}{2(\gamma-1)}} \tag{22}$$

A second assumption is that the boundary-layer shape parameter H defined as

$$H = \frac{\delta^*}{\theta} \tag{23}$$

has a constant value of 1.4 as in reference 7.

Having established C_D and δ_T^* simultaneous solution of equations (6c), (22), and (23) will yield values for unknowns M_E, δ_E^*, and θ_E if the free-stream Mach number at the effective throat section is assumed to equal unity.

It is now possible to solve for throat pressure from

$$\frac{P_T}{P_E} = \left(\frac{1 + \frac{\gamma - 1}{2} M_E^2}{1 + \frac{\gamma - 1}{2} M_T^2} \right)^{\frac{\gamma}{\gamma - 1}} \tag{24}$$

and to form the ratio P_T/P_H for comparison with the same ratio found for the runs with $\frac{L}{D} = 0$ from equation (4).

Temperature and velocity in the effective throat may now be found from equations (5a), (7), and (8).

Duct losses may be lumped into coefficient form by basing a thrust coefficient, as defined in equation (9), on geometrical throat area.

Similarly, boundary-layer effects on the mass rate of flow may be summed up in the form of a pipe discharge coefficient by using geometrical throat area in equation (11).

Because of the erosion discussed previously, the variation of pipe cross-sectional area with time is an unknown. Only initial and final measured areas are available. In addition, somewhere during each run the pressure tap at the exit station closed up due to metal flow. Values of measured exit pressure were reliable only during approximately the initial 0.1 second of burning. In view of these two factors, solving for throat pressure, using the equations just outlined, was possible only for a point early in each run, 0.05 second, where the pipe diameter was assumed to still have its original unfired value[3] and where exit pressure was known. The time 0.05 second was arbitrarily picked for all runs since by then ignition effects seemed to have been dissipated and orderly burning initiated.

Instantaneous mass-flow rates were found at 0.05 second from equation (17) having measured the original burning surface prior to each run

---

[3]Firings of similar tailpipes with thermocouples installed yielded values of inside wall temperature at 0.05 second of the order of 700° F. It is unlikely that temperatures of this order of magnitude could have caused metal flow. Correction for thermal expansion of the pipes proved negligible.

and assuming that its variation with time followed a pattern determined from the runs with $\frac{L}{D} = 0$ for the particular propellant configuration concerned.

It is thus evident that for the tailpipe runs the ratio P_T/P_H was established at a point early in each run. The error involved in employing this method, rather than one based on values of quantities averaged over the entire run, will be small if changes in skin-friction and heat-transfer coefficients as the heat content of the pipe walls increases are not significant.

Using the equations and assumptions outlined, the following quantities which are completely independent of all variables except L/D may be found for each run: for the runs with $\frac{L}{D} = 0$, thrust coefficient, discharge coefficient, specific impulse, and the ratio P_T/P_H; for the tailpipe runs, pipe discharge coefficient, throat displacement thickness, and the ratios P_T/P_H and δ_T^*/L.

Once having established these fundamental quantities, they were used with the same equations to recompute all performance changes of interest to the designer under a set of equivalent conditions for all runs, L/D being the only variable. Unit geometrical throat area, an expended propellant weight of 10 pounds, and 200 square inches of burning surface were used for all cases,[4] and throat conditions were made equal to exit conditions.

RESULTS AND DISCUSSION

Table III lists the values of the quantities found for each run which are independent of variables other than L/D. It will be seen that runs of similar L/D show excellent agreement. Hence, what at first seemed to indicate rather widely scattered experimental results may be attributed to the unavoidable injection of extraneous variables into the investigation in the form of powder grain differences and nozzle erosion.

The recalculated performance characteristics, for a standard set of conditions, using averages of the basic quantities shown in table III,

---

[4]These values were picked only to arrive at pressures, thrusts, and so forth of the same order of magnitude as obtained experimentally. Unit values of all quantities could have been used just as well.

are presented in table IV. These represent the only true comparison that can be made, for all expended propellant weights and burning surfaces are the same, and expansion takes place only up to throat conditions. Any change in performance is solely a function of tailpipe length.

The designer will undoubtedly never use a high-pressure tailpipe without incorporating an expansion cone, so these quantities do not represent the absolute values expected for a practical application. However, since what occurs after the throat section is independent of the length of a high-pressure tailpipe, a comparison of values between the different L/D's is indicative of the net change to be expected. In view of this, figures 7 to 11 show the percent change with L/D of the various performance characteristics. These percentages are based on the values obtained for a zero-length tailpipe.

It will be seen from figure 7 that boundary-layer development causes reductions in the effective throat area which, in turn, increase the value of the ratio K. The immediate effect of this change in K is to effect a percentage change of chamber head pressure of almost four times the percent change of K. This is a direct result of the value of n in the exponent of equation (18a) being equal to 0.73 for the powder used, JPN. Depending on the value of n, it may be seen that slight changes in K may result in considerable changes in pressure.

An immediate effect of the increase in chamber pressure is evident from figure 8. Higher chamber pressures with accompanying higher burning rates result in shorter burning times and increased mass-flow rates.

Figure 9 illustrates the effect of duct losses. Friction and heat transfer reduce the ratio P_T/P_H as well as the temperature, and hence velocity, in the effective throat.

Figure 10 shows the change in total thrust as well as its components, momentum thrust, and pressure thrust. Despite the duct losses shown in figure 9, it can be seen from this figure that the increase in operating pressure because of throat reduction completely overwhelms the losses and considerable increases in thrust are obtained. Much larger increases in pressure thrust than in momentum thrust are noted. This leads one to believe that heat losses, with their attendant lowering of temperatures and hence jet momentum, may play a more significant role in tailpipe losses than does skin friction. Figure 10 also indicates the effect of pipe losses in reducing total and specific impulse.

Pipe thrust and discharge coefficients which sum up in coefficient form the effect of duct losses are presented in figure 11.

Figure 12 shows that the value of the ratio δ_T^*/L decreases with tailpipe length. This effect may be explained if for purposes of discussion the simplified assumption is made that the ratio δ_T^*/L is defined as for a flat plate in incompressible flow (ref. 8)

$$\frac{\delta_T^*}{L} \approx \frac{k}{(R_e)^{1/5}} \tag{25}$$

where k is a constant. For longer tailpipes, and therefore greater heat extraction, temperatures and viscosities at the throat section will decrease. This will increase the Reynolds number and consequently reduce δ_T^*/L. It thus appears possible that with enough heat extraction boundary-layer thickness may be reduced despite longer pipe lengths available for its growth.

Changes in rocket performance due to varying high-pressure tailpipe length have been investigated for a particular propellant composition having given powder and gas constants. The percent change in the ratio P_T/P_H and the ratio δ_T^*/L will vary with L/D according to figures 9 and 12, respectively, for most rocket gases having similar Reynolds numbers. It will be seen, therefore, that using the equations outlined and these two basic quantities (plus an experimental discharge coefficient established from reference runs) the designer may evaluate performance changes to be expected by increasing the tailpipe length of any given rocket-propellant combination.

CONCLUSIONS

The following conclusions may be drawn from the experimental investigation of the effect of high-pressure tailpipe length on the performance of solid-propellant motors for rocket-powered aircraft:

1. Development of boundary-layer results in a reduction of effective throat area for mass flow from its $\frac{L}{D} = 0$ value for increasing tailpipe lengths. This reduction amounts to 3.3 percent for $\frac{L}{D} = 5$, 5.1 percent for $\frac{L}{D} = 10$, 6.4 percent for $\frac{L}{D} = 15$.

2. These changes in effective throat area result in increases in the ratio K, for a constant propellant configuration of 3.5 percent for $\frac{L}{D} = 5$, 5.4 percent for $\frac{L}{D} = 10$, and 6.8 percent for $\frac{L}{D} = 15$.

3. For a propellant with a burning rate exponent n of 0.73, the increases in the ratio K result in increases of chamber head pressure of 13.4 percent for $\frac{L}{D} = 5$, 21.4 percent for $\frac{L}{D} = 10$, and 27.6 percent for $\frac{L}{D} = 15$.

4. Increases in operating pressure with resultant higher burning rates reduce the burning time by 8.8 percent for $\frac{L}{D} = 5$, 13.2 percent for $\frac{L}{D} = 10$, and 16.3 percent for $\frac{L}{D} = 15$.

5. Shorter burning times with a fixed amount of propellant to be consumed result in increases in mass-flow rate of 9.6 percent for $\frac{L}{D} = 5$, 15.2 percent for $\frac{L}{D} = 10$, and 19.5 percent for $\frac{L}{D} = 15$.

6. Friction and heat-transfer losses reduce the ratio of throat to chamber head pressure by 3.2 percent for $\frac{L}{D} = 5$, 4.1 percent for $\frac{L}{D} = 10$, and 4.9 percent for $\frac{L}{D} = 15$. Temperature in the effective throat is reduced by 6.3 percent for $\frac{L}{D} = 5$, 8.0 percent for $\frac{L}{D} = 10$, and 9.5 percent for $\frac{L}{D} = 15$. The corresponding drop in velocity is 3.2 percent for $\frac{L}{D} = 5$, 4.1 percent for $\frac{L}{D} = 10$, and 4.9 percent for $\frac{L}{D} = 15$.

7. Pipe losses are completely overwhelmed by the increases in chamber pressure and resultant increases in thrust of 6.4 percent for $\frac{L}{D} = 5$, 10.9 percent for $\frac{L}{D} = 10$, and 14.2 percent for $\frac{L}{D} = 15$ are obtained.

8. The losses become apparent in causing reductions in total and specific impulse of 3.0 percent for $\frac{L}{D} = 5$, 3.7 percent for $\frac{L}{D} = 10$, and 4.4 percent for $\frac{L}{D} = 15$.

9. Summing up boundary-layer effects in coefficient form results in:

(a) A reduction of a pipe thrust coefficient of 6.2 percent for $\frac{L}{D} = 5$, 8.6 percent for $\frac{L}{D} = 10$, and 10.5 percent for $\frac{L}{D} = 15$

(b) A reduction of a pipe discharge coefficient of 3.3 percent for $\frac{L}{D} = 5$, 5.1 percent for $\frac{L}{D} = 10$, and 6.4 percent for $\frac{L}{D} = 15$

10. The effect of greater heat extraction for longer tailpipes is to reduce the rate of growth of throat displacement thickness by approximately 24 percent for $\frac{L}{D} = 10$ and 37 percent for $\frac{L}{D} = 15$ based on the value obtained for $\frac{L}{D} = 5$.

11. From these results, it may be concluded that high-pressure tailpipe lengths in the L/D range investigated may have marked effects on solid-propellant rocket performance. Performance changes, though not radically affected by friction, may be significantly altered by the reduction in effective throat area caused by the boundary layer buildup. The large increases in chamber pressure obtained for even a small throat reduction make this factor of special importance in cases where peak chamber pressures must be controlled for structural considerations.

Langley Aeronautical Laboratory
National Advisory Committee for Aeronautics
Langley Field, Va.

APPENDIX

DERIVATION OF EQUATION (21) FOR MOMENTUM THRUST DEFICIENCY

In this derivation the following symbols, in addition to those previously defined, apply:

y	distance normal to pipe axis
δ	boundary-layer thickness
ρ_y	variable density in y-direction (a variable only in the boundary layer)
V_y	variable velocity in y-direction (a variable only in the boundary layer)

As before, ρ and V are free-stream (constant) density and velocity, respectively. The following diagram refers to a symmetrical round pipe. The origin of the y-axis is taken at the center line of the pipe.

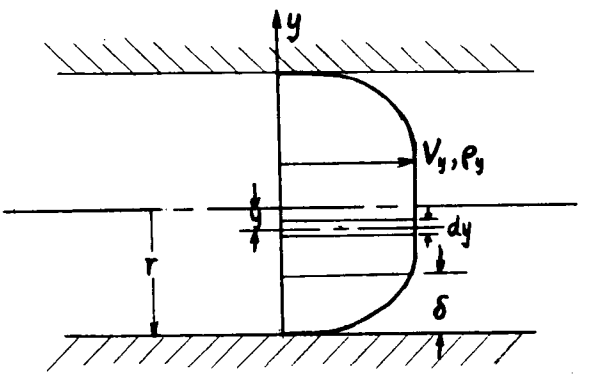

For the case in question, the displacement thickness may be defined as (referring to the diagram)

$$\delta^* = \int_r^{r-\delta} \left(1 - \frac{\rho_y V_y}{\rho V}\right)\frac{y}{r}\, dy$$

and the momentum thickness as

$$\theta = \int_r^{r-\delta} \frac{\rho_y V_y}{\rho V}\left(1 - \frac{V_y}{V}\right)\frac{y}{r}\, dy$$

Momentum thrust deficiency = (Momentum thrust if density and velocity were constant across pipe and equal to free-stream values) - (Actual momentum thrust with density and velocity variable)

$$-\Delta\dot{m}V = \rho V^2 \pi r^2 - \int_0^r \rho_y V_y{}^2 2\pi y\, dy$$

Considering the second term of the right-hand side of the above equation, it may be rewritten as

$$\int_0^r \left(\rho V^2 \frac{\rho_y V_y{}^2}{\rho V^2} - \rho V^2 \frac{\rho_y V_y}{\rho V} + \rho V^2 \frac{\rho_y V_y}{\rho V} - \rho V^2 + \rho V^2\right) 2\pi y\, dy$$

which may be rearranged as

$$\int_0^r \left\{-\rho V^2 \left[\frac{\rho_y V_y}{\rho V}\left(1 - \frac{V_y}{V}\right)\right] - \rho V^2\left(1 - \frac{\rho_y V_y}{\rho V}\right) + \rho V^2\right\} 2\pi y\, dy$$

Expanding integration limits

$$\rho V^2\left[-\int_0^{r-\delta}\frac{\rho_y V_y}{\rho V}\left(1-\frac{V_y}{V}\right)2\pi y\,dy-\int_{r-\delta}^{r}\frac{\rho_y V_y}{\rho V}\left(1-\frac{V_y}{V}\right)2\pi y\,dy-\right.$$

$$\left.\int_0^{r-\delta}\left(1-\frac{\rho_y V_y}{\rho V}\right)2\pi y\,dy-\int_{r-\delta}^{r}\left(1-\frac{\rho_y V_y}{\rho V}\right)2\pi y\,dy+\int_0^{r}2\pi y\,dy\right]$$

In interval of integration between 0 and $r - \delta$, $\rho_y = \rho$, and $V_y = V$, so that integrands for these limits become zero.

Rewriting, and multiplying and dividing first and second terms by r, the expression becomes

$$\rho V^2\left[-2\pi r\int_{r-\delta}^{r}\frac{\rho_y V_y}{\rho V}\left(1-\frac{V_y}{V}\right)\frac{y}{r}\,dy-2\pi r\int_{r-\delta}^{r}\left(1-\frac{\rho_y V_y}{\rho V}\right)\frac{y}{r}\,dy+2\pi\int_0^{r}y\,dy\right]$$

as

$$\int_{r-\delta}^{r}\frac{\rho_y V_y}{\rho V}\left(1-\frac{V_y}{V}\right)\frac{y}{r}\,dy=-\int_{r}^{r-\delta}\frac{\rho_y V_y}{\rho V}\left(1-\frac{V_y}{V}\right)\frac{y}{r}\,dy$$

The expression may be rewritten as

$$\rho V^2(2\pi r\theta+2\pi r\delta^*+\pi r^2)$$

The momentum thrust deficiency is then

$$-\Delta\dot{m}V=\rho V^2\pi r^2-\rho V^2 2\pi r\theta-\rho V^2 2\pi r\delta^*-\rho V^2\pi r^2$$

or

$$\Delta\dot{m}V=\rho V^2 2\pi r(\delta^*+\theta)$$

REFERENCES

1. Hagginbothom, W. K., and Thibodaux, J. G.: Aerodynamic Losses in Low-Pressure Tailpipe Exhaust Ducts for Rocket-Propelled Aircraft. NACA RM L8C25, 1948.

2. Anon.: Rocket Fundamentals. OSRD No. 3992, ABL-SR4, NDRC, Div. 3, Sec. H, 1944.

3. Mahon, H. I., Noland, R. L., Rogers, W. L., Sanders, V., and Schoafsma, W.: Investigation of Internal-Burning Grain Configurations. Progress Rep. No. 985/7-12 (Contract NOa(S)9767), Aerojet Eng. Corp., Aug. 9, 1949.

4. Wolfe, H. L.: Investigation of M2 (T28) Jato with High Pressure Duct between Chamber and Nozzle. Picatinny Arsenal Rep. No. 1 Project No. TU2-2011A, Serial No. 1735, June 9, 1949.

5. Sage, B. H.: Some Studies of the Internal Ballistics of Jet-Propelled Devices. Rep. No. A-115: Progress Rep., OSRD-1069, NDRC, 1942.

6. Noland, R. L., Rogers, W. L., Roth, E., and Springer, D. F.: Investigation of Aeroplex Propellants and Metal Components for Booster Rockets. Pts. II and III. Rep. No. 336 (Contract NOa(S) 9382), Aerojet Eng. Corp., Dec. 7, 1948.

7. Young, A. D., and Winterbottom, N. E.: High Speed Flow in Smooth Cylindrical Pipes of Circular Section. Rep. No. Aero 1785, British R.A.E., Nov. 1942.

8. Prandtl, L.: The Mechanics of Viscous Fluids. Turbulent Flow Along a Wall With Special Reference to the Frictional Resistance of Plates. Vol. III of Aerodynamic Theory, div. G, sec. 23, W. F. Durand, ed., Julius Springer (Berlin), 1935, pp. 145-154.

TABLE I

POWDER CONSTANTS FOR JPN PROPELLANT FROM REFERENCE 2

Coefficient in burning rate equation for 70° F firing temperature, c (fig. 6-1)	0.0044
Exponent in burning rate equation, n (table 6-1)	0.73
Corrected density of propellant, ρ', lb/in.^{3} (table 6-1 and ch. 3)	0.0586
Ratio of specific heats for exhaust gases, γ (calculated as per appendix 8)	1.22
Gas constant for exhaust gases, R, ft/°R (ch. 2)	57.6

NACA

TABLE II

SUMMARY OF CERTAIN EXPERIMENTAL RESULTS

Quantity	$\frac{L}{D}$ = 0, first test	$\frac{L}{D}$ = 0, second test	$\frac{L}{D}$ = 0, third test	$\frac{L}{D}$ = 5, first test	$\frac{L}{D}$ = 5, second test	$\frac{L}{D}$ = 10, first test	$\frac{L}{D}$ = 10, second test	$\frac{L}{D}$ = 15, first test	$\frac{L}{D}$ = 15, second test
Initial grain weight, lb	9.75	9.80	9.74	9.99	9.80	9.83	9.69	9.83	9.84
Initial burning surface, sq in.	203.3	203.0	205.4	204.3	200.9	199.9	201.8	203.3	204.5
Initial A_T, sq in.	1.099	1.099	1.099	1.099	1.099	1.099	1.099	1.099	1.099
Final A_T, sq in.	1.197	1.180	1.178	1.181	1.179	1.160	1.142	1.120	1.123
w, lb	9.56	9.60	9.54	9.79	9.60	9.63	9.49	9.63	9.65
t_b, sec	1.030	1.065	1.055	0.980	1.000	0.945	0.892	0.880	0.795
I, lb-sec	1633	1641	1630	1694	1657	1652	1603	1678	1695
I_S, sec	170.9	170.9	170.8	173.1	172.5	171.5	168.8	174.2	175.7
Av. $\bar{m}$, lb/sec	9.28	9.02	9.05	9.99	9.60	10.19	10.64	10.95	12.14
Av. F, lb	1585	1541	1545	1729	1657	1748	1797	1907	2132
Av. P_H, lb/sq in. abs	1146	1130	1129	1308	1259	1363	1423	1528	1692
Av. P_N, lb/sq in. abs	1119	1108	1107	1282	1231	1334	1396	1501	1663
Check on expansion									
F at 0.05 sec, lb	1421	1417	1469	1531	1425	1483	1523	1640	1690
P_H at 0.05 sec, lb/sq in. abs	1055	1052	1087	1204	1120	1188	1222	1330	1369
F/A_TP_H at 0.05 sec	1.225	1.225	1.230	1.156	1.157	1.135	1.133	1.121	1.122
F at t_b, lb	1330	1393	1394	1555	1424	1405	1693	1796	2162
P_H at t_b, lb/sq in. abs	907	969	970	1090	1002	1020	1296	1375	1652
F/A_TP_H at t_b	1.225	1.218	1.220	1.208	1.206	1.188	1.144	1.166	1.166

NACA

TABLE III

QUANTITIES FOUND EXPERIMENTALLY WHICH ARE DEPENDENT ONLY ON $\frac{L}{D}$

(a) For reference runs.

Quantity	$\frac{L}{D}$ = 0, first test	$\frac{L}{D}$ = 0, second test	$\frac{L}{D}$ = 0, third test
C_F	1.231	1.231	1.231
C_D	0.00720	0.00721	0.00721
I_S, sec	170.9	170.9	170.8
$\frac{P_T}{P_H}$	0.5611	0.5611	0.5611

(b) For tailpipe runs.

Quantity	$\frac{L}{D}$ = 5, first test	$\frac{L}{D}$ = 5, second test	$\frac{L}{D}$ = 10, first test	$\frac{L}{D}$ = 10, second test	$\frac{L}{D}$ = 15, first test	$\frac{L}{D}$ = 15, second test
C_D	0.00696	0.00697	0.00684	0.00684	0.00674	0.00673
δ_T^*, in. . .	0.0099	0.0098	0.0150	0.0152	0.0187	0.0191
$\frac{\delta_T^*}{L}$, $\frac{\text{in.}}{\text{in.}}$ . . .	0.00168	0.00166	0.00127	0.00128	0.00105	0.00107
$\frac{P_T}{P_H}$	0.5424	0.5438	0.5387	0.5376	0.5338	0.5338

TABLE IV

RECALCULATED PERFORMANCE CHARACTERISTICS BASED ON AVERAGES OF THE QUANTITIES LISTED IN TABLE III AND A STANDARD SET OF CONDITIONS: UNIT GEOMETRICAL THROAT AREA, 10 POUNDS OF EXPENDED PROPELLANT WEIGHT, 200 SQUARE INCHES OF BURNING SURFACE, AND NO EXPANSION BEYOND THROAT CONDITIONS

Quantity	$\frac{L}{D} = 0$	$\frac{L}{D} = 5$	$\frac{L}{D} = 10$	$\frac{L}{D} = 15$
δ_T^*/L, in./in.	0	0.00167	0.00128	0.00106
δ_T^*, in.	0	0.0094	0.0144	0.0179
A_T', in.^{2}	1.000	0.967	0.949	0.936
K	200.0	206.9	210.8	213.6
P_H, lb/sq in. abs	1378	1563	1673	1758
$\bar{\dot{m}}$, lb/sec	9.93	10.89	11.44	11.86
t_b, sec	1.007	0.919	0.874	0.843
P_T/P_H	0.5611	0.5431	0.5382	0.5338
C_F	1.233	1.157	1.127	1.104
C_D, sec^{-1}	0.00721	0.00697	0.00684	0.00674
F, lb	1700	1808	1886	1941
I, lb-sec	1712	1661	1648	1637
I_S, sec	171.2	166.1	164.8	163.7
T_T, $^\circ$R	4126	3866	3796	3735
V_T, ft/sec	3052	2954	2927	2903
Momentum thrust, lb	941	974	1000	1017
Pressure thrust, lb	759	834	886	924

NACA

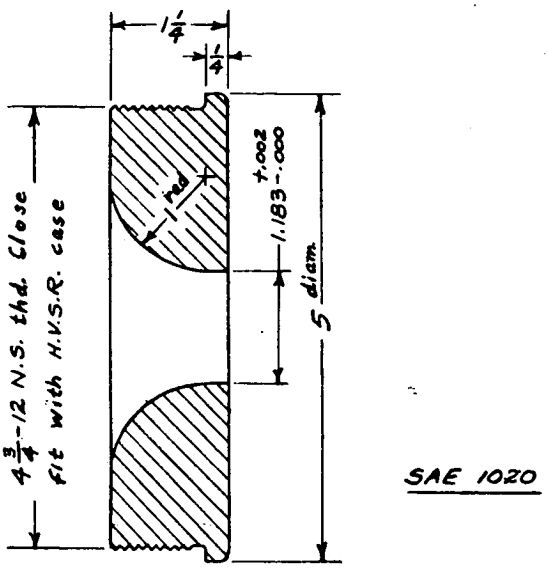

(a) Convergent nozzle for reference run, $\frac{L}{D} = 0$.

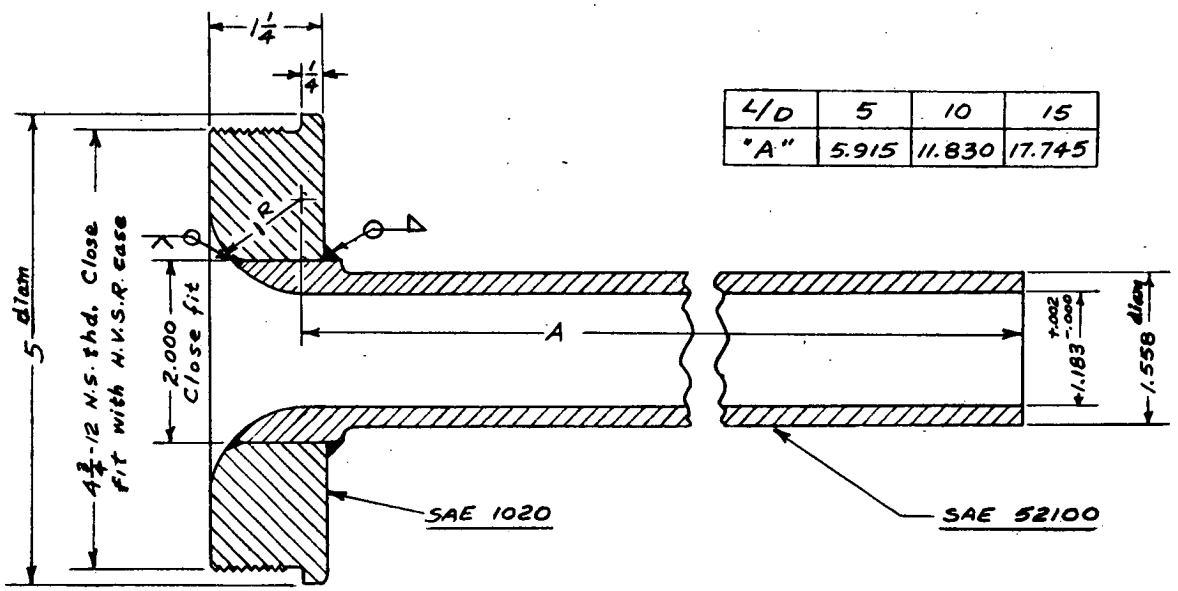

(b) High-pressure tailpipes, $\frac{L}{D} = 5, 10, 15$.

Figure 1.- Test configurations. All dimensions are in inches.

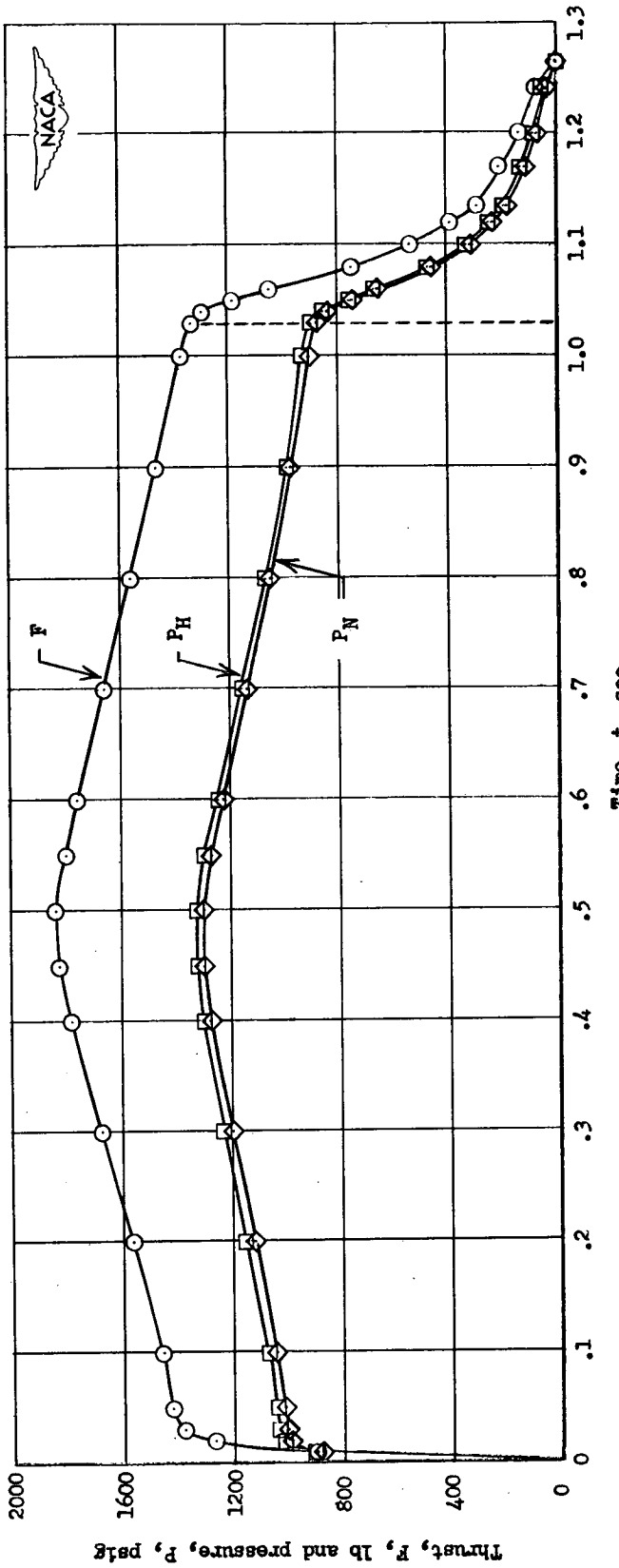

Figure 2.- Variation of thrust and pressure with time for reference run.
$\frac{L}{D} = 0.$

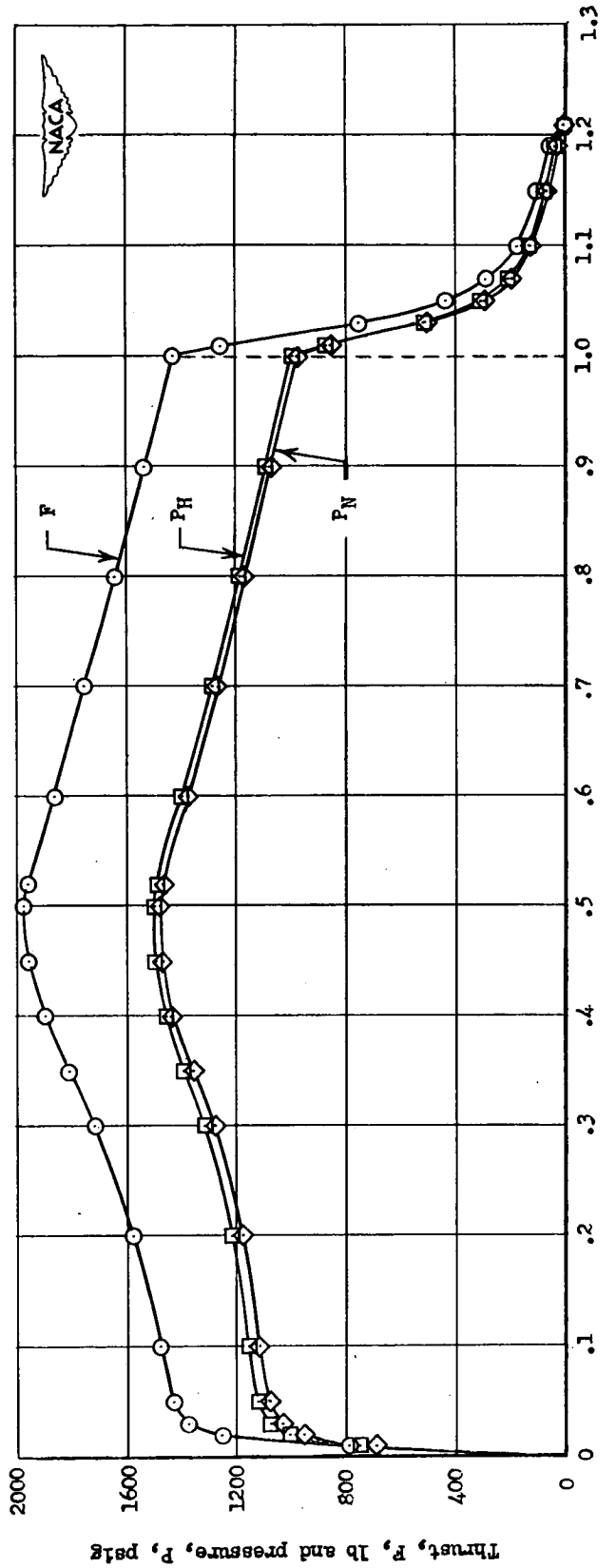

Figure 3.- Variation of thrust and pressure with time for high-pressure tailpipe run. $\frac{L}{D} = 5$.

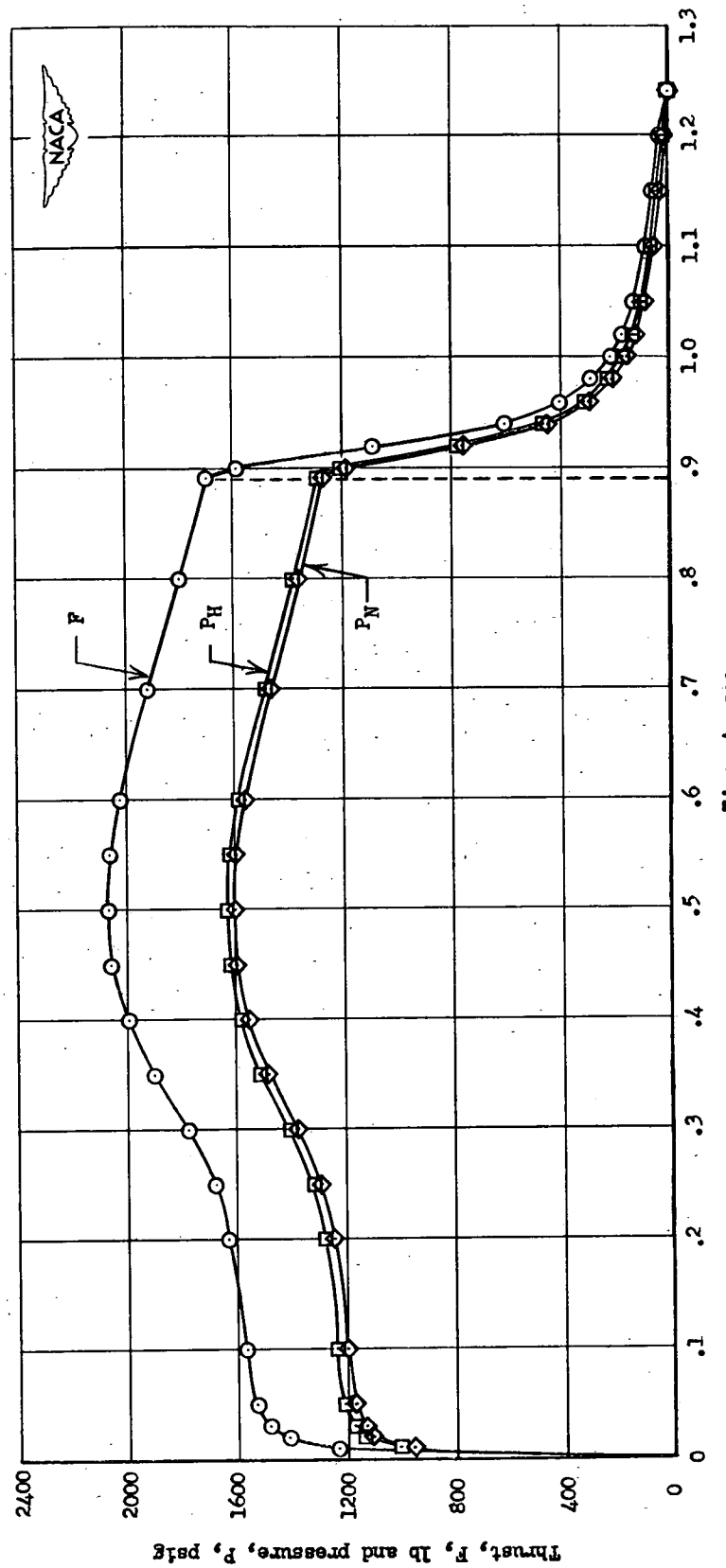

Figure 4.- Variation of thrust and pressure with time for high-pressure tailpipe run. $\frac{L}{D} = 10$.

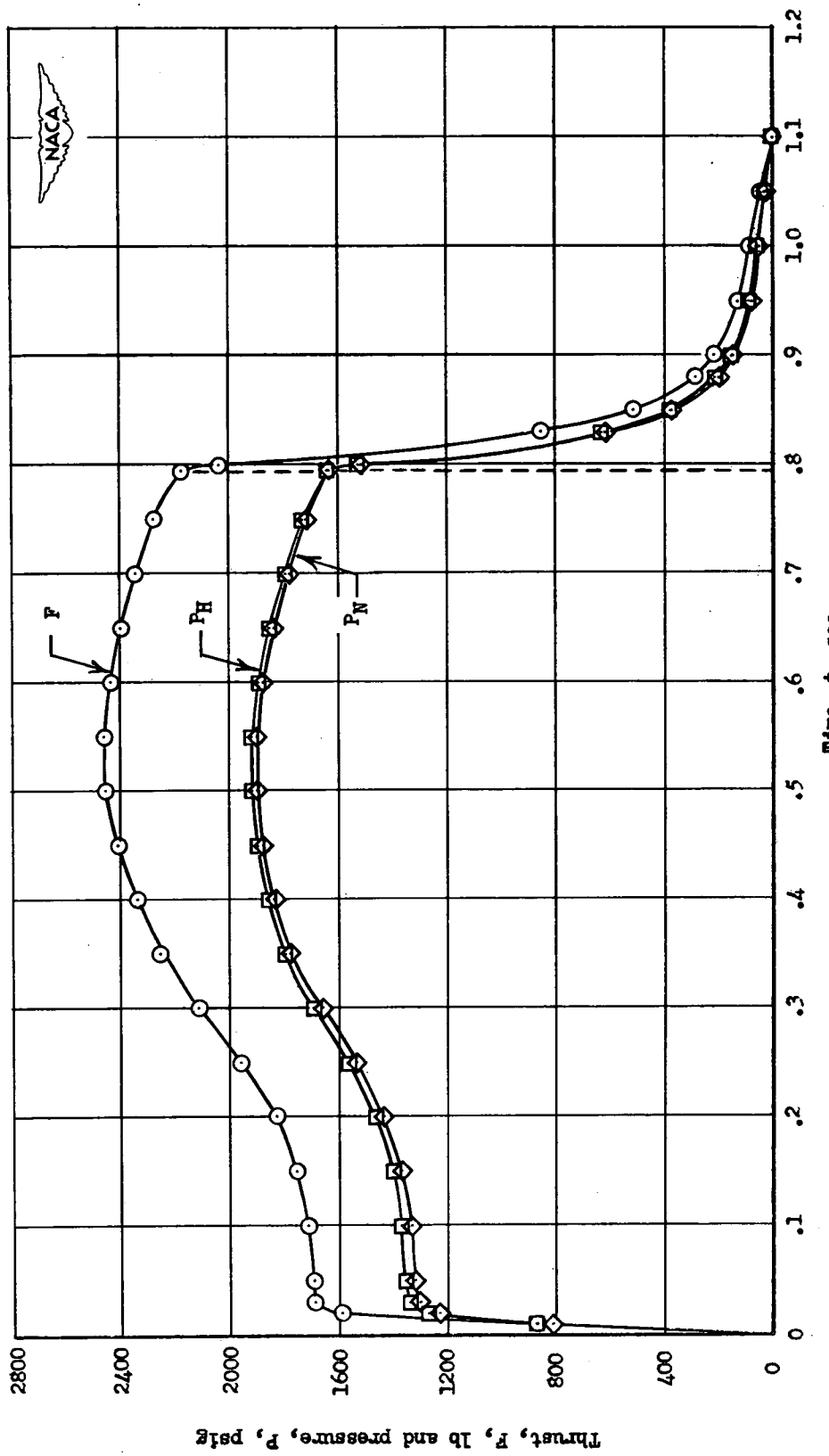

Figure 5.- Variation of thrust and pressure with time for high-pressure tailpipe run. $\frac{L}{D} = 15$.

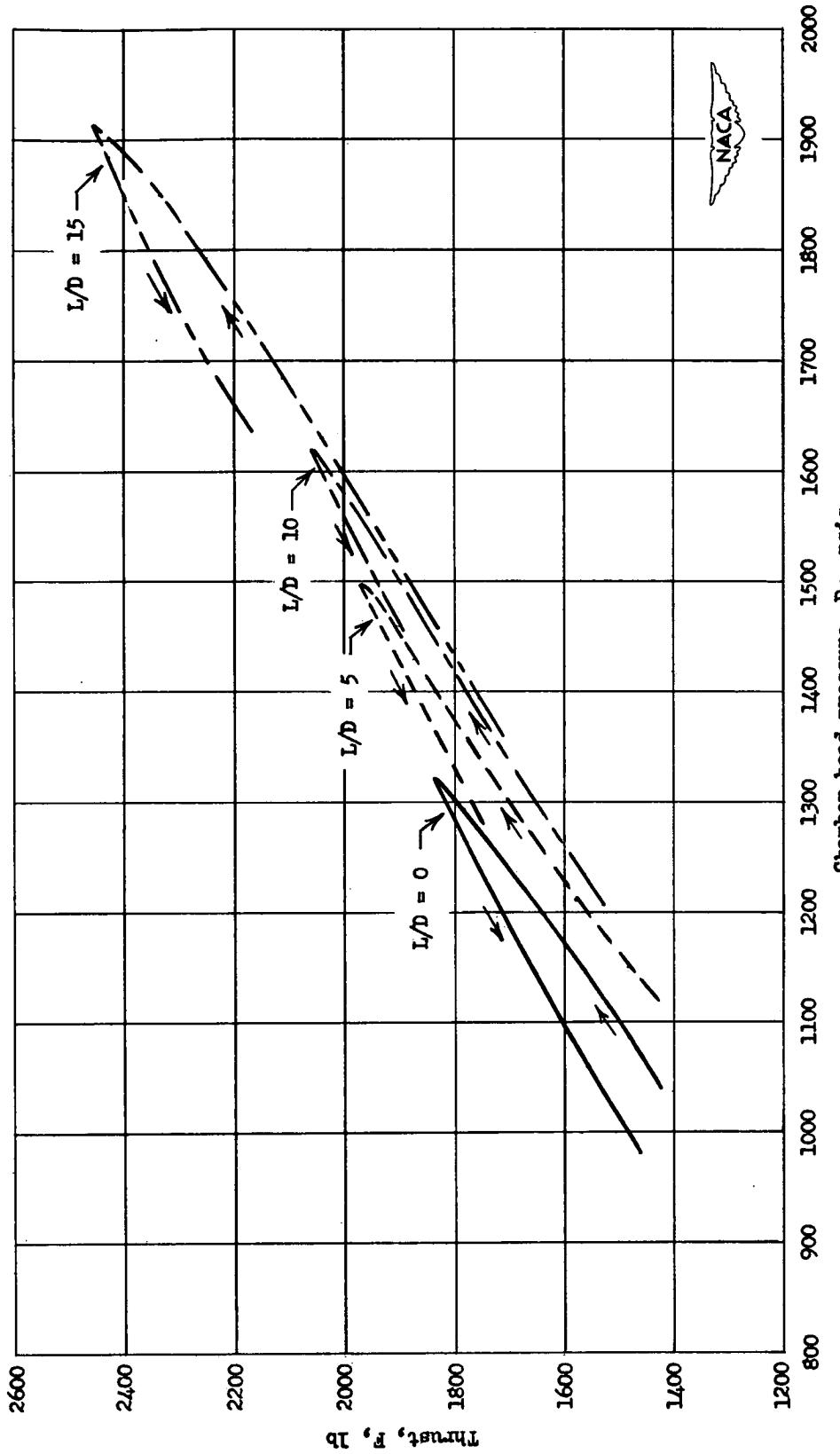

Figure 6.- Variation of thrust with chamber head pressure for $\frac{L}{D}$ = 0, 5, 10, 15.

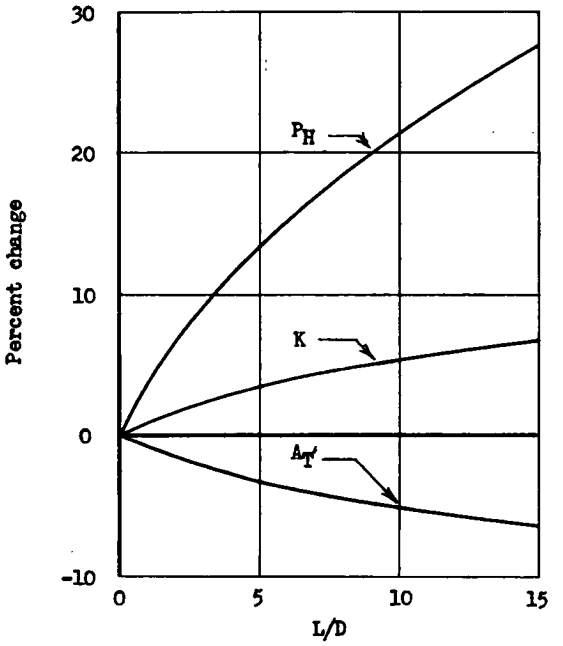

NACA

Figure 7.- Percent change with L/D of effective throat area, K ratio, chamber head pressure.

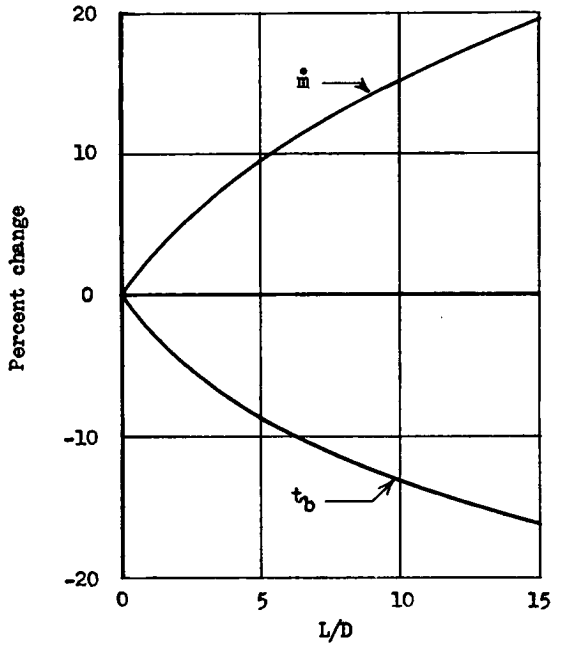

NACA

Figure 8.- Percent change with L/D of mass rate of flow, burning time.

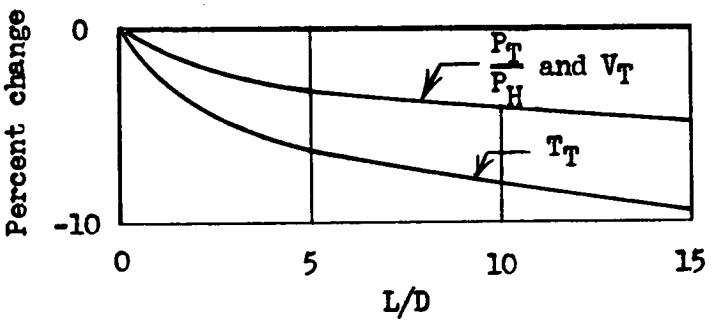

Figure 9.- Percent change with L/D of pressure ratio, and temperature and velocity in effective throat.

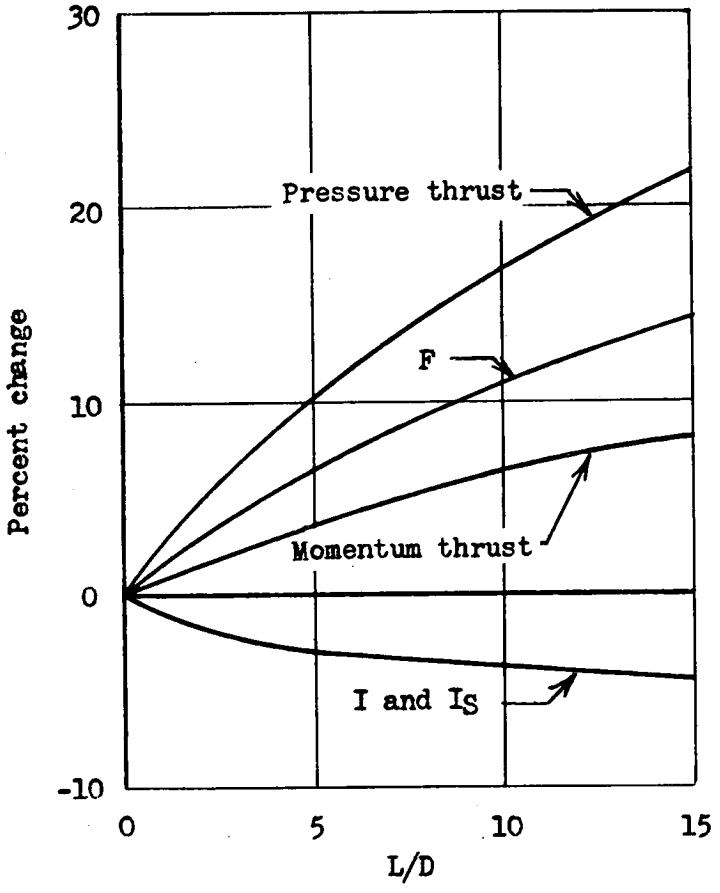

Figure 10.- Percent change with L/D of total thrust and its components, and total and specific impulse.

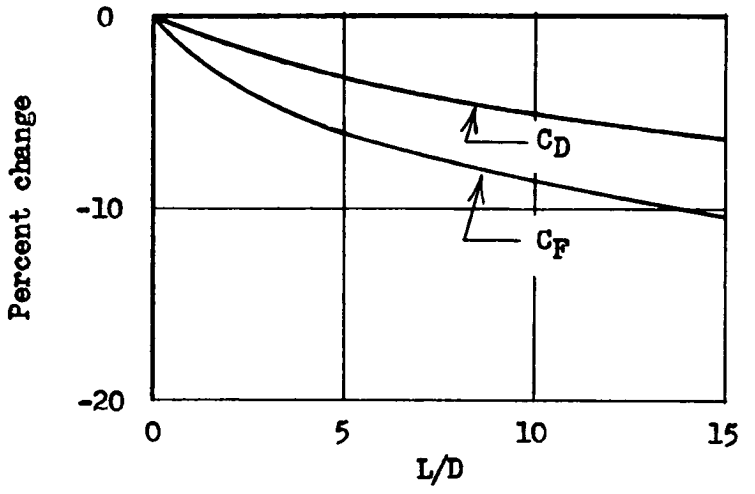

Figure 11.- Percent change with L/D of pipe thrust and discharge coefficients based on geometrical throat area.

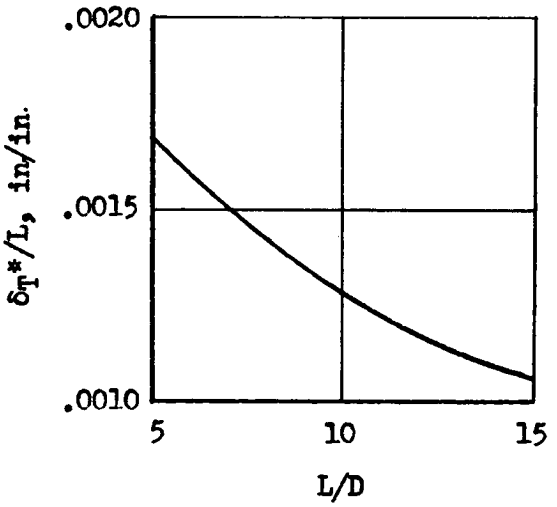

Figure 12.- Change in rate of growth of displacement thickness at throat section with L/D.